Neurobiology of Disease 42 (2011) 506–513

Contents lists available at ScienceDirect

Neurobiology of Disease

journal homepage: www.elsevier.com/locate/ynbdi

Cx32 and Cx47 mediate oligodendrocyte:astrocyte and oligodendrocyte: oligodendrocyte gap junction coupling

Sameh K. Wasseff *, Steven S. Scherer *

Department of Neurology, University of Pennsylvania School of Medicine, Philadelphia, PA, USA

ARTICLE INFO

Article history:
Received 1 March 2011
Accepted 2 March 2011
Available online 8 March 2011

Keywords:
Oligodendrocyte
Astrocyte
Gap junctions
Connexins

ABSTRACT

In addition to the extensive gap junction coupling between astrocytes themselves, oligodendrocytes are thought to be exclusively coupled to astrocytes (O:A coupling) via heterotypic gap junctions composed of Cx47:Cx43 and Cx32:Cx30. We used fluorescent dyes to examine functional coupling in acute slices from the cerebra of mice lacking Cx32 and/or Cx47. In the corpus callosum, unexpectedly, oligodendrocytes appeared to be directly and exclusively coupled to other oligodendrocytes (O:O coupling), and electron microscopy revealed gap junctions between adjacent oligodendrocytes. O:O coupling was more affected in mice lacking Cx32 than in mice lacking Cx47. In the neocortex, oligodendrocytes appeared to be directly and exclusively coupled to astrocytes; Cx47, but not Cx32, was required for O:A coupling.

Introduction

Connexins (Cx) are a family of ~20 genes that encode the proteins that form gap junctions (GJs) in vertebrates (Sohl and Willecke, 2004). Each GJ is an aggregate composed of tens of thousands of individual channels, each of which is composed of two apposed hemichannels on adjacent cell membranes (Kumar and Gilula, 1996). Most cell types express one or more Cxs, including astrocytes, which are extensively coupled by GJs. Astrocytes are coupled to each other (A:A coupling) by Cx43:Cx43 and Cx30:Cx30 homotypic channels, and are thought to be coupled to oligodendrocytes (O:A coupling) by heterotypic Cx47:Cx43 and Cx32:Cx30 channels (Altevogt and Paul, 2004a; Li et al., 2004; Nagy and Rash, 2003; Nagy et al., 2003a; Orthmann-Murphy et al., 2007b, 2008; Rash et al., 2001a,b). Oligodendrocytes are not thought to be directly coupled by GJs (Mugnaini, 1986), although Cx32 probably forms GJs that link the layers of the myelin sheath (Kamasawa et al., 2005).

Mutations in *GJB1*, the gene that encodes Cx32, cause X-linked Charcot–Marie–Tooth (CMT1X), the second most common kind of inherited demyelinating neuropathy (Kleopa and Scherer, 2006). In addition to slowed conduction in peripheral nerves, many patients also have slowed central conduction, and a subset of patients develop overt CNS manifestations including spasticity, hyperreflexia, ataxia, and acute reversible encephalopathy with white matter abnormalities on MRI (Akimoto et al., 2010; Bahr et al., 1999; Kleopa et al., 2002, 2006; Nicholson and Corbett, 1996; Nicholson et al., 1998; Panas et al., 2001; Paulson et al., 2002; Siskind et al., 2009; Takashima et al., 2003; Taylor et al., 2003; Zambelis et al., 2008). Recessive mutations in *GJC2*, the gene encoding Cx47, cause Pelizaeus–Merzbacher-like disease (PMLD), a severe leukodystrophy with childhood onset, characterized by nystagmus, progressive spasticity, and ataxia (Bugiani et al., 2006; Uhlenberg et al., 2004).

These human diseases demonstrate that Cx32 and Cx47 play essential roles in the maintenance of oligodendrocytes/CNS myelin, and this has been affirmed in the analysis of mice with loss of function mutations in both *Gjb1* (encodes mouse Cx32) and *Gjc2* (encodes mouse Cx47). These "double-null" mice develop a variety of pathological findings, including vacuoles, demyelination, and apoptotic oligodendrocytes (Menichella et al., 2003, 2006; Odermatt et al., 2003). In this paper, we wished to determine the relative contributions of Cx32:Cx30 and Cx47:Cx43 to O:A coupling by examining the extent of dye transfer in young wild-type, *Gjb1*-null, *Gjc2*-null, and double-null mice. Because O:A coupling is lost in the neocortex and the corpus callosum of double-null mice, Cx32 and Cx47 are required for O:A coupling, presumably because both Cx32:Cx30 and Cx47:Cx43 GJs are absent. Because O:A coupling is lost in the neocortex of *Gjc2*-null mice, but not in *Gjb1*-null mice, it is likely mediated mainly through Cx47:Cx43 channels. In the corpus callosum, O:A coupling is not seen, even in wild-type mice. Rather, we find O:O coupling that is partially disrupted in *Gjb1*-null mice, but not in *Gjc2*-null mice, so it is likely mediated mainly through Cx32:Cx32 channels. Electron microscopy, furthermore, demonstrates that oligodendrocytes are directly coupled by GJs.

* Corresponding authors at: University of Pennsylvania Department of Neurology, 464 Stemmler Hall, 3450 Hamilton Walk, Philadelphia, PA 19104–6077.
E-mail addresses: swasseff@mail.med.upenn.edu (S.K. Wasseff), sscherer@mail.med.upenn.edu (S.S. Scherer).

Available online on ScienceDirect (www.sciencedirect.com).

0969-9961/$ – see front matter © 2011 Elsevier Inc. All rights reserved.
doi:10.1016/j.nbd.2011.03.003

Methods

Animals

All experiments were conducted according to University of Pennsylvania guidelines for laboratory animal use. *Gjb1*-null mice (Nelles et al., 1996) were obtained from Dr. David Paul at Harvard University, and have been maintained on a C57BL/6 background. *Gjc2*-null mice, in which oligodendrocytes express EGFP (Odermatt et al., 2003), were obtained from the European Mouse Mutant Archive in Italy and maintained on a B6; 129 background.

Electrophysiology

All recordings and images were conducted using an Olympus BX51WI fixed stage microscope, fitted with a 40× water immersion objective with a long working distance, infrared differential interference contrast (IR-DIC), and videomicroscopy through an Olympus DP-71 color camera using DP-71 software. The images imaging had a green fluorescent background, which was much higher in *Gjc2* mutant mice (heterozygous and null) than in wild type mice, and was strongest in the white matter, owing to the abundance of EGFP positive oligodendrocytes in this region. The whole cell recordings were conducted using a Model 2400 amplifier (A-M Systems); signals were digitized using National Instruments USP interface card, and analyzed using WCP software (version 3.6 up to version 4.0.7, John Dempster, Department of Physiology & Pharmacology, Strathclyde Institute for Biomedical Sciences, University of Strathclyde, Scotland).

Acute brain slices were prepared from post-natal day 14 (P14) to P40 mice; typically pairs of mice that were genetically distinct, but from the same litter, were analyzed on consecutive days, because a single experiment typically took an entire day. The mice were anesthetized, decapitated, and the cerebrum was dissected, immersed for 5 min in oxygenated (bubbled with 95% O_2-5%CO_2), ice-cold artificial cerebrospinal fluid (ACSF) composed of 238 or 250 mM sucrose, 2.5 mM KCl, 1.0 mM NaH_2PO_4, 1.3 mM $MgSO_4$, 2.5 mM $CaCl_2$, 11 mM dextrose, and 26.2 mM $NaHCO_3$ (pH 7.4, 295–305 mOsm), and sectioned horizontally into 200 μm thick sections using a Leica VT1000S vibratome. Slices were incubated in oxygenated ACSF (119 or 125 mM NaCl, 2.5 mM KCl, 1.mM NaH_2PO_4, 1.3 mM $MgSO_4$, 2.5 mM $CaCl_2$, 11 mM dextrose, and 26.2 mM $NaHCO_3$ with a pH of 7.4 and an osmolarity of 295–305 mOsm) for 1 h, then placed in the recording chamber continuously perfused at a rate 2 ml/min with 100% O_2 bubbled ACSF. For Sulforhodamine-101 labeling, the sections were incubated immediately after sectioning in 0.1% Sulforhodamine-101 in ACSF for 20 min (Kafitz et al., 2008). Electrodes were filled with an intracellular solution composed of 105 mM K-gluconate, 30 mM KCL, 0.3 mM EGTA, 10 mM HEPES, 10 mM phosphocreatine, 4 mM ATP-Mg_2, 0.3 mM GTP-Tris, with 0.1% Sulforhodamine-B (SR-B; MW 559; Invitrogen), Lucifer Yellow (LY; MW 457; Sigma) or 0.5% biocytin (BC; MW 372; Sigma) adjusted to a pH of 7.4 with KOH. EGFP-positive cells that had regular, visible surface on IR-DIC were patched, and were observed over 1–20 min in current-clamp mode. These EGFP-positive cells had the same passive electrophysiological characteristics of oligodendrocytes as previously reported (Odermatt et al., 2003) with a RMP of -71.6 ± 8.1 mV. Cells that displayed RMP less than -50 mV were discarded. For biocytin labeling experiments, oligodendrocytes were patched for 20 min and then sections were immediately fixed in 4% paraformaldehyde overnight at 4 °C, then blocked for 1 h in a blocking solution (0.1% Triton X-100, 5% fish skin gelatin in PBS), and incubated for 48 h at 4 °C with Cy5-conjugated strepavidin (1:200 dilution; Jackson ImmunoResearch Laboratories). Slides were mounted with Vectorshield, and examined by epifluorescence with appropriate optical filters by an epifluorescent Leica DMR microscope, using interactive software (MetaMorph; Leica). Statistical analysis was carried out using Fisher's exact test for categorical outcome; coupling versus uncoupling. Subsequently the Wilcoxon rank sum test was used to determine whether there is a statistically significant difference in the number of coupled cells between groups in which coupling was seen.

Electron microscopy

P22 mice were transcardially perfused with 2.5% glutaraldehyde in 0.1 M PB, the cerebra were dissected, cut into ~1 mm thick coronal sections, fixed overnight at 4 °C, then osmicated, dehydrated, and embedded in Epon. Transverse semithin sections (0.5 μm) were mounted on glass slides and stained with alkaline toluidine blue. Thin sections (90 nm thick) were mounted on 2 × 1 mm single-slot, formvar-coated grids, stained with lead citrate and uranyl acetate, and examined with a JOEL 1200 electron microscope. Oligodendrocytes and astrocytes were identified by their ultrastructural feature (Peters et al., 1991). Oligodendrocytes had electron-dense cytoplasm with abundant rough endoplasmic reticulum and no intermediate filaments; cells with these morphological characteristics were found in continuity with myelin sheaths. They were typically found in rows, these included "light" oligodendrocytes (Imamoto et al., 1978). Astrocytes had electron-lucent cytoplasm that contained intermediate filaments and glycogen; cells with these morphological characteristics were found adjacent to blood vessels.

Results

Cx47:Cx43, but not Cx32:Cx30, channels are required for O:A coupling in the neocortex

To investigate O:A coupling in the brain, we examined *Gjc2*-null ($Gjc2^{-/-}$) mice (which lack Cx47) and their heterozygous ($Gjc2^{+/-}$) littermates. Because the *Egfp* gene replaces the *Gjc2* gene in these mice, the fluorescence of EGFP can be used as a marker of oligodendrocytes as rigorously shown by Odermatt et al. (2003). To label astrocytes, we incubated slices of cerebra for 20 min in Sulphorhodamine-101 (SR-101; MW 607 Da; uncharged), as previously described (Kafitz et al., 2008). As shown in Fig. 1A, SR-101 labeled stellate cells that were about 50 μm apart in the neocortex. Isolated, EGFP-positive oligodendrocytes were present throughout the neocortex, especially in the deeper layers (III–VI), and were most abundant in the corpus callosum, where their cell bodies typically formed intrafascicular rows parallel to the myelinated axons. In the neocortex of both $Gjc2^{-/-}$ and $Gjc2^{+/-}$ mice, SR-101-positive astrocytes were labeled as soon as we examined the slices (after 20 min), and the labeling was maintained for the duration of the experiment. In the deeper layers of the neocortex, almost all oligodendrocytes in $Gjc2^{+/-}$ mice were SR-101-positive after 1 hour, whereas in $Gjc2^{-/-}$ mice, SR-101-positive oligodendrocytes were not seen even after 6–8 h. We obtained these results on 3–5 slices/mouse, from 3 pairs of $Gjc2^{-/-}$ mice and their $Gjc2^{+/-}$ littermates sacrificed at one of three ages (P14–15, P21–22, and P27–P29). We did not see SR-101-positive oligodendrocytes in the corpus callosum of either $Gjc2^{-/-}$ mice or $Gjc2^{+/-}$ mice, but it is difficult to interpret this finding because SR-101-positive astrocytes were quite sparse.

These results indicate that Cx47 is required for the diffusion of SR-101 between astrocytes and oligodendrocytes in the cortex, likely via O:A junctions composed of Cx47:Cx43. To test this idea, we patched EGFP-positive cells in the sections described above, 1–5 h after incubation with SR-101, with electrodes containing Lucifer Yellow (LY; MW 457 Da, -2). We patched single EGFP-positive cells that were within 50 μm of at least two SR-101-positive cells. In $Gjc2^{+/-}$ mice, LY diffused into SR-101-positive cells in 5/7 cases (Fig. 1B; upper panels). By contrast, in $Gjc2^{-/-}$ mice, LY diffused into SR-101-positive cells in 0/7 cases (Fig. 1B; lower panels). The two groups are statistically different by Fisher's exact test ($p < 0.021$). These results, taken together, demonstrate bidirectional diffusion of small molecules between astrocytes and oligodendrocytes.

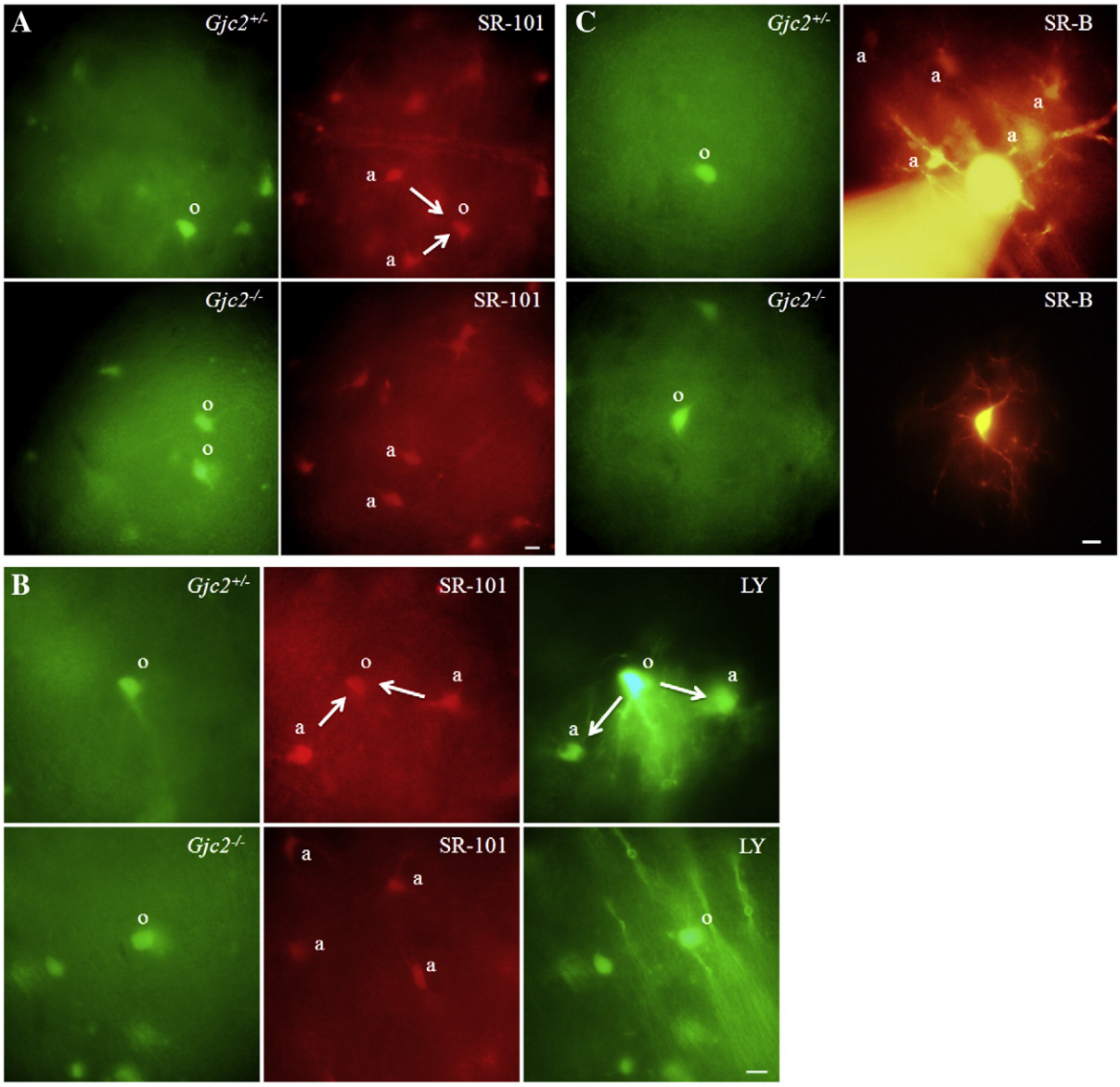

Fig. 1. Cx47 is required for A:O coupling in the neocortex. These are digital images of layers III–VI from sections of the neocortex from P14–P30 *Gjc2*$^{-/-}$ mice (which lack Cx47) or their *Gjc2*$^{+/-}$ littermates. The sections were imaged with FITC, to visualize EGFP or Lucifer Yellow (LY), and TRITC, to visualize Sulforhodamine-101 (SR-101) or Sulforhodamine-B (SR-B). Note that following injection of LY (panel B) or SR-B (panel C), the processes of the glial cells are prominently labeled, in addition to the soma. Scale bars: 10 μm. A&B. Astrocytes (a; the non-EGFP-positive cells) have been labeled by incubating the slices in artificial cerebrospinal fluid containing SR-101 for 20 min. In panel A, note that the SR-101 also labels EGFP-positive oligodendrocytes (o) as SR-101 diffused from astrocytes (a) to oligodendrocytes (o) as indicated by arrows in *Gjc2*$^{+/-}$ mice (upper panels), but not in their *Gjc2*$^{-/-}$ littermates, indicating that Cx47 is required for the transfer of SR-101 from astrocytes to oligodendrocytes. In panel B, a single EGFP-positive oligodendrocyte (o) was injected with LY, and then imaged for 20 min. In *Gjc2*$^{+/-}$ mice (upper panels), but not in *Gjc2*$^{-/-}$ mice (lower panels), notice that the SR-101 positive astrocytes (a) became LY-positive, as LY diffused from oligodendrocytes (o) to astrocytes (a) as indicated by arrows, indicating that Cx47 is required for bidirectional GJ coupling between astrocytes and oligodendrocytes. The spread of LY into the processes of the injected oligodendrocyte results in a more extensive FITC signal. C. An EGFP-positive oligodendrocyte was injected with SR-B and visualized for 20 min. In *Gjc2*$^{+/-}$ mice (upper panels), but not in *Gjc2*$^{-/-}$ mice (lower panels), SR-B diffused into EGFP-negative cells (presumably astrocytes; a), indicating that Cx47 is required for the diffusion of SR-B.

As an independent test, we used a different fluorescent dye, Sulforhodamine-B (SR-B, 559 Da, uncharged), which has been previously shown to cross A:A GJs (Rouach et al., 2008). We patched EGFP-positive cells in layers III–VI in a separate set of P19–P30 *Gjc2*$^{-/-}$ and *Gjc2*$^{+/-}$ mice. As shown in Fig. 1C, in *Gjc2*$^{+/-}$ mice, SR-B labeled stellate, EGFP-negative cells that we presume to be astrocytes. In all *Gjc2*$^{-/-}$ mice, SR-B labeled only the injected cell. Because Cx32:Cx30 channels are minimally permeable to LY (Orthmann-Murphy et al., 2007b), and perhaps other dyes, one might argue that the lack of O:A coupling seen in *Gjc2*$^{-/-}$ mice owes to a minimum permeability of Cx32:Cx30 channels to SR-B. To evaluate this possibility, we used biocytin (BC), a smaller (MW 372 Da, uncharged) and a more permeant tracer (Houades et al., 2008), and found that BC, too, did not diffuse from EGFP-positive oligodendrocytes to surrounding EGFP-negative cells in *Gjc2*$^{-/-}$ mice. To perform this experiment, we selected regions of the neocortex (layers III–VI) that had an isolated EGFP-positive cell, which was patched for 20 min before being processed to visualize biocytin. All 6 sections (from 3 different P14–P31 *Gjc2*$^{-/-}$ mice) that were successfully processed contained only one biocytin-positive cell. Fig. 2 shows one example. In contrast, all 3 sections (from 3 different *Gjc2*$^{+/-}$ mice) had multiple biocytin-positive cells, which we presume to be astrocytes because they were EGFP-negative.

As an additional test of whether Cx32:Cx30 mediates O:A coupling in the neocortex, we examined a separate set of P22–P25 *Gjb1*-null

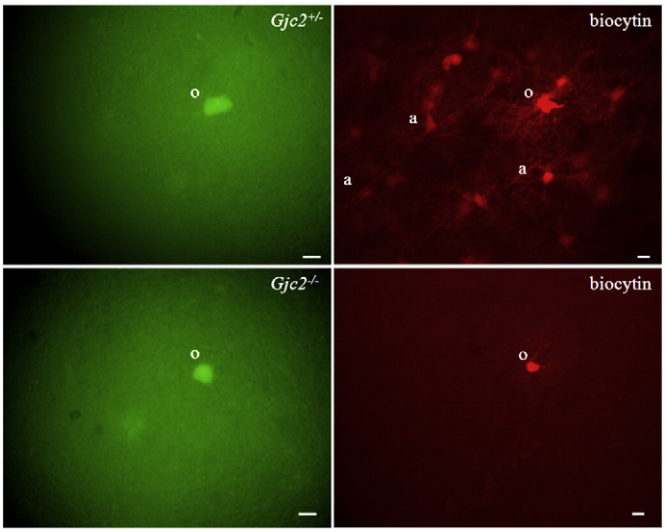

Fig. 2. No O:A coupling in $Gjc2^{-/-}$ neocortex. These are digital images of layers III–VI from sections of the neocortex from P14–P31 $Gjc2^{-/-}$ mice (which lack Cx47) or their $Gjc2^{+/-}$ littermates. We selected fields containing one well isolated EGFP-positive cell (o), which was patched with an electrode containing biocytin for 20 min. The section was fixed and incubated in Cy5-conjugated streptavidin to visualize the biocytin. Notice that biocytin diffused to surrounding EGFP-negative cells (presumably astrocytes; a) in $Gjc2^{+/-}$ mice, but remained localized to the injected cell in $Gjc2^{-/-}$ mice. Scale bars: 10 μm.

mice (which lack Cx32) in a $Gjc2^{+/-}$ background (so that we could still visualize oligodendrocytes). We patched EGFP-positive cells in layers III–VI with electrodes containing SR-B. As shown in Fig. 3, SR-B labeled stellate, EGFP-negative cells (presumably astrocytes) in both $Gjb1^{-/Y}//Gjc2^{+/-}$ and $Gjb1^{+/Y}//Gjc2^{+/-}$ mice, further demonstrating that O:A coupling is independent of Cx32. Taken together, these data

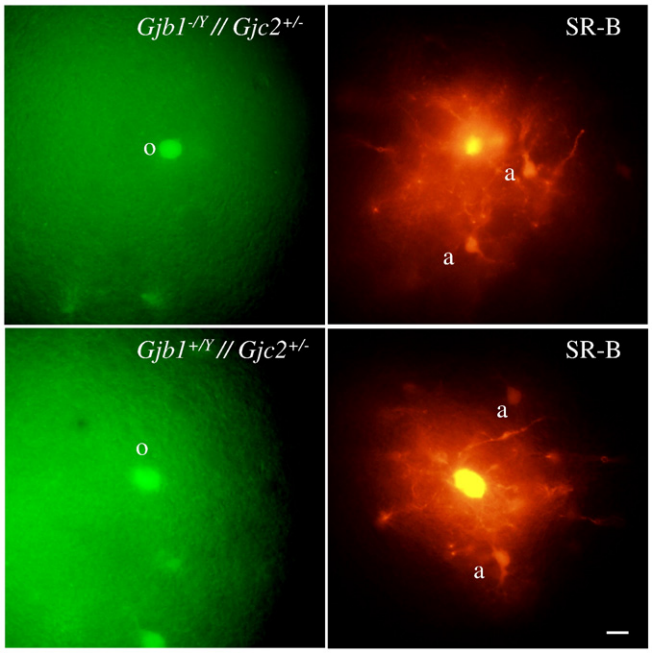

Fig. 3. Cx32 is not required for the O:A coupling in neocortex. These are digital images of layers III–VI from sections of the neocortex from P22–P25 $Gjb1^{-/Y}//Gjc2^{+/-}$ mice (which lack Cx32) or their $Gjb1^{+/Y}//Gjc2^{+/-}$ littermates. An EGFP-positive oligodendrocyte (o) was patched with an electrode containing SR-B for 20 min, then the sections were imaged for TRITC to visualize SR-B. Note that SR-B prominently labels the processes of the injected oligodendrocytes, and also labels the soma of non-EGFP-positive cells, presumably astrocytes (a) in both $Gjb1^{-/Y}//Gjc2^{+/-}$ (upper panels) and $Gjb1^{+/Y}//Gjc2^{+/-}$ mice (lower panels). Scale bar: 10 μm.

demonstrate that O:A coupling in the neocortex is mediated by Cx47:Cx43; we find no evidence of functional Cx32:Cx30 channels.

Cx32 is more important than Cx47 for GJ coupling in the corpus callosum

We similarly examined the corpus callosum, motivated by the documented heterogeneity of astrocytes (Emsley and Macklis, 2006; Haas et al., 2006; Houades et al., 2006; Matyash and Kettenmann, 2010), including the heterogeneity of connexin expression by both astrocytes and oligodendrocytes (see Introduction). We patched EGFP-positive cells in the corpus callosum in slices from P22–P29 $Gjc2^{-/-}$ mice ($n=4$) and their $Gjc2^{+/-}$ littermates ($n=3$) with electrodes containing SR-B. After 20 min, we observed SR-B in multiple cells in every slice. Further, all of the SR-B-positive cells appeared to be EGFP-positive, demonstrating that they were oligodendrocytes. Fig. 4A shows one example from each genotype. While our work was in progress, Maglione et al. (2010) reported that GJ coupling was less extensive in the corpus callosum of $Gjc2^{-/-}$ mice than in $Gjc2^{+/-}$ mice. Our quantitative analysis of injected cells, however, did not reveal a significant difference in the number of SR-B labeled cells between these two genotypes ($p>0.05$, Wilcoxon rank sum test; Table 1).

The above findings demonstrate that oligodendrocytes in the corpus callosum are extensively coupled by GJs, and that Cx47 is not essential for this coupling. We therefore examined the possibility that Cx32:Cx30 GJs mediate this coupling by labeling EGFP-positive cells in slices from $Gjb1^{-/Y}//Gjc2^{+/-}$ mice ($n=8$) and their $Gjb1^{+/Y}//Gjc2^{+/-}$ littermates ($n=5$). As illustrated in Fig. 4B, SR-B labeling was restricted to the injected cell in 13/20 sections from $Gjb1^{-/Y}//Gjc2^{+/-}$ mice; 7 sections had 2–10 labeled cells. In contrast, only 2/11 sections from the $Gjb1^{+/Y}//Gjc2^{+/-}$ mice had a single labeled cell; 9/11 sections had multiple labeled cells (2–13 cells). This difference is significant by the Wilcoxon rank sum test ($p<0.05$); Table 2. According to this analysis, Cx32 is more important for GJ coupling than is Cx47 in the corpus callosum.

These findings indicate that oligodendrocytes in the corpus callosum are directly coupled by GJs, as we did not see labeled astrocytes. To examine the possibility that astrocytic processes mediate this apparent O:O coupling ("O:A:O coupling"; Rash et al., 2001a,b), we examined interfasicular oligodendrocytes in thin sections of the corpus callosum from three different P22 mice using electron microscopy. An intervening cytoplasmic process was not seen between 12 apposed pairs of oligodendrocytes. Moreover, we identified GJs between more than one-half of these cell pairs; an example is shown in Fig. 5A. We observed similar GJs between astrocytes (Fig. 5B). Thus, in contrast to the prevailing view (see Introduction), many oligodendrocytes are directly coupled to other oligodendrocytes.

Loss of both Cx32 and Cx47 abolishes oligodendrocyte coupling

The persistence of oligodendrocyte coupling in the corpus callosum of $Gjc2^{-/-}$ mice noted above could be owed to the presence of an additional unidentified connexin, or perhaps a previously reported up-regulation of Cx32 along myelinated fibers (Li et al., 2008). Furthermore, $Gjb1^{-/Y}//Gjc2^{-/-}$ double-null mice exhibit much more severe dysmyelination and motor abnormalities than do $Gjc2^{-/-}$- or $Gjb1^{-/Y}$-single-null mice (Menichella et al., 2003; Odermatt et al., 2003). Thus, we wished to determine whether GJ coupling was completely disrupted in $Gjb1^{-/Y}//Gjc2^{-/-}$ mice ($n=4$; P24–P30). We patched EGFP-positive cells in the neocortex and corpus callosum with electrodes containing SR-B. As illustrated in Fig. 6, SR-B labeling was always restricted to the injected cell, indicating that GJ coupling in the corpus callosum (5/5 patched cells) and the neocortex (5/5 patched cells) was totally absent. These findings confirm that Cx47 and Cx32 are the only connexins responsible for O:A and O:O coupling in young mice.

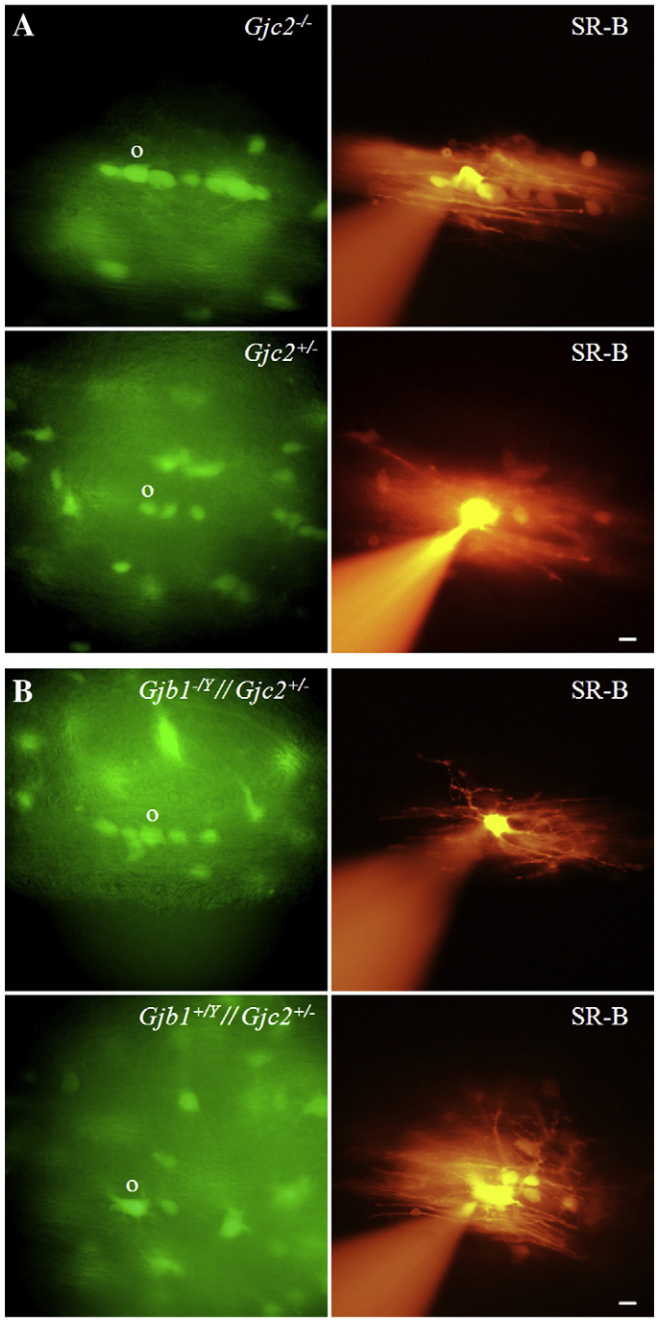

Fig. 4. GJ coupling is diminished in the corpus callosum of *Gjb1*-null mice. These are digital images of the corpus callosum from sections of P22–P29 $Gjc2^{-/-}$ mice (which lack Cx47) or their $Gjc2^{+/-}$ littermates (Panel A), or $Gjb1^{-/Y}//Gjc2^{+/-}$ mice (which lack Cx32) or their $Gjb1^{+/Y}//Gjc2^{+/-}$ littermates (panel B). An EGFP-positive (FITC filters) oligodendrocyte (o) was patched with an electrode containing SR-B and visualized (TRITC filters) after 20 min. Note that the SR-B prominently labels the processes of injected cells. Scale bars: 10 μm. A. In the both the $Gjc2^{-/-}$ (upper panels) and $Gjc2^{+/-}$ mice (lower panels), SR-B diffused into surrounding EGFP-positive oligodendrocytes up to 100 μm away. B. In $Gjb1^{-/Y}//Gjc2^{+/-}$ mice (upper panels), unlike $Gjb1^{+/Y}//Gjc2^{+/-}$ mice (lower panels), SR-B did not diffuse into surrounding EGFP-positive oligodendrocytes.

Discussion

GJ coupling in the corpus callosum

The finding that oligodendrocytes appear to be coupled only to other oligodendrocytes in the corpus callosum (our results and those of Maglione et al., 2010) is at odds with the traditional view that oligodendrocytes are only coupled to astrocytes (Mugnaini, 1986; Rash et al., 2001a,b). The initial failure to find O:A or O:O coupling (Berger et al., 1991; Butt and Ransom, 1989; Pastor et al., 1998; Ransom and Kettenmann, 1990) may be owed to the low pH in the pipette solution (7.2) and the fact that LY does not cross Cx32:Cx30 channels (Orthmann-Murphy et al., 2007b). Other findings also conflict with this traditional view: labeling astrocytes in the corpus callosum with biocytin did not label oligodendrocytes (Haas et al., 2006; Matyash and Kettenmann, 2010), deleting both Cx43 and Cx30 did not abolish biocytin diffusion between oligodendrocytes (Maglione et al., 2010), and electron microscopic data confirming that oligodendrocytes are directly coupled by GJs (see below).

Whether O:O coupling is mediated mostly by Cx32:Cx32 or by Cx47:Cx47 homotypic channels remains to be determined. Maglione et al. (2010) patched oligodendrocytes with biocytin (visualized with strepavidin-Cy3), and found fewer labeled cells in $Gjc2^{-/-}$ mice than in wild type mice, similar numbers of labeled cells in *Gjb1*-null mice as in wild type mice, and no biocytin transfer in double-null mice. Using SR-B, we found similar numbers of cells in the corpus callosum of $Gjc2^{-/-}$ and $Gjc2^{+/-}$ mice, fewer cells in $Gjb1^{-/Y}//Gjc2^{+/-}$ mice than in $Gjb1^{+/Y}//Gjc2^{+/-}$mice, and no coupled cells in double-null mice (Tables 1 and 2). Thus, while we agree on the most fundamental result—that glial GJ coupling in the corpus callosum is lost in double-null mice—our results differ from those of Maglione et al. (2010) in that we find evidence of disrupted GJ coupling in $Gjb1^{-/Y}$ mice, whereas they find disrupted GJ coupling in $Gjc2^{-/-}$ mice.

The reasons for these discrepancies are unclear. Both Cx32- and Cx47-positive GJ plaques are found in the corpus callosum (Kleopa et al., 2004), and the dramatically worse phenotype of double-null mice, as compared to mice lacking either Cx32 or Cx47 alone, demonstrates that these two connexins partially compensate for the loss of each other (Menichella et al., 2003; Odermatt et al., 2003). Some technical considerations are worth considering. First, the lower number of labeled cells in our experiments likely reflects the lower sensitivity of SR-B as compared to biocytin. Accordingly, we think that the SR-B labeled cells are probably the most strongly coupled cells in the more extensive network of coupled cells quantified by Maglione et al. (2010). Second, we always used $Gjc2^{+/-}$ mice as controls, rather than wild type mice, because we wanted to exploit the EGFP signal in selecting

Table 1
Cx47 is not essential for Sulforhodamine-B dye transfer in the corpus callosum. The number (mean ± S.D.) of SR-B-labeled cells per slice in the corpus callosum of individual P22–P29 $Gjc2^{-/-}$ and $Gjc2^{+/-}$ mice is shown. There is no significant difference between the two genotypes ($p > 0.05$, Wilcoxon rank sum test).

n	$Gjc2^{-/-}$	$Gjc2^{+/-}$
1	8.0 ± 4.2 (2 sections)	7.0 ± 2.7 (3 sections)
2	6.0 ± 6.9 (3 sections)	5.5 ± 5.0 (2 sections)
3	5.0 ± 0.0 (2 sections)	3 (1 section)
4	10.0 ± 4.0 (3 sections)	–
Mean	7.4 ± 4.5	5.8 ± 3.2

Table 2
Cx32 is essential for normal Sulforhodamine-B dye transfer in the corpus callosum. The number (mean ± S.D.) of SR-B-labeled cells per slice in the corpus callosum of individual P22–P29 mice is shown. There were significantly more SR-B-labeled cells per slice in $Gjb1^{+/Y}//Gjc2^{+/-}$ mice than in $Gjb1^{-/Y}//Gjc2^{+/-}$ mice ($p > 0.05$, Wilcoxon rank sum test).

n	$Gjb1^{-/Y}//Gjc2^{-/-}$	$Gjb1^{+/Y}//Gjc2^{+/-}$
1	0 ± 0.0 (3 sections)	5.0 ± 1.4 (2 sections)
2	0 ± 0.0 (3 sections)	1.7 ± 2.1 (3 sections)
3	5 (1 section)	4.7 ± 7.2 (3 sections)
4	3.3 ± 4.7 (4 sections)	3.0 ± 2.8 (2 sections)
5	1.5 ± 0.7 (2 sections)	3 (1 section)
6	1.3 ± 2.3 (2 sections)	–
7	0 ± 0.0 (2 sections)	–
8	1.5 ± 2.1 (2 sections)	–
Mean	1.0 ± 2.6	3.5 ± 3.8

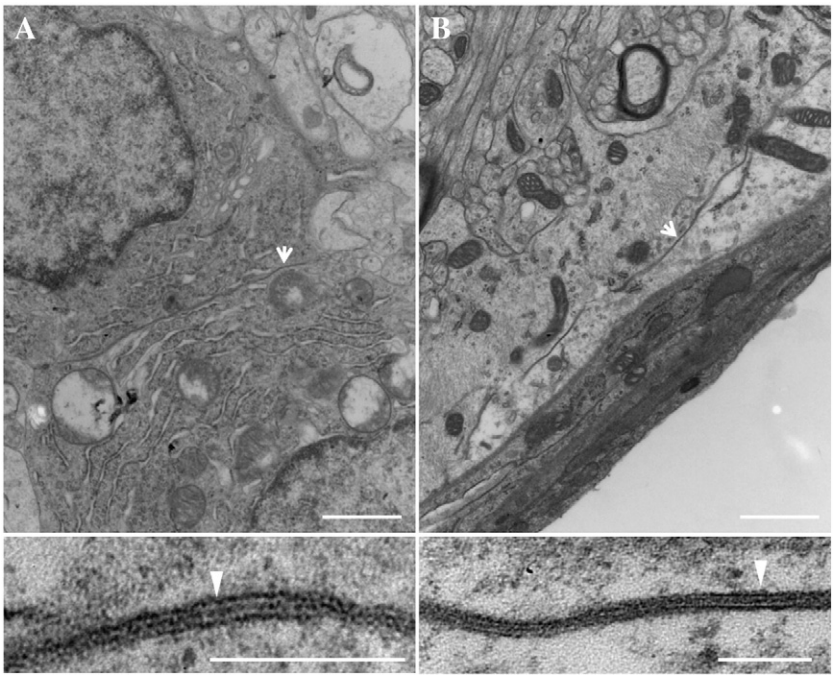

Fig. 5. O:O junctions between interfascicular oligodendrocytes. These are digital electron micrographs from coronal thin sections of the corpus callosum from P22 mice. The upper image in panel A shows a pair of oligodendrocytes, which can be recognized by their electron-dense cytoplasm and well-developed rough endoplasmic reticulum. The two cells are directly apposed, with no intervening processes. The region indicated by the arrow is shown at higher magnification in the lower panel; this image shows an extensive GJ (arrowhead). The upper image in panel B shows a pair of astrocytic processes (recognized by their electron-lucent cytoplasm that contains intermediate filaments) that are adjacent to a blood vessel. The region indicated by the arrow is shown at higher magnification in the lower panel; this image shows an extensive GJ (arrowhead). Scale bars: 1 μm in both upper panels; 100 nm in both lower panels.

cells to patch, and it is possible that halving the dose of *Gjc2* reduces GJ coupling. Third, it is possible that some of the "oligodendrocytes" that were patched in wild type mice by Maglione et al. (2010) were not, in fact, oligodendrocytes, as when these authors patched EGFP-positive cells, biocytin only labeled EGFP-positive cells, in accord with our finding that all SR-B-positive cells in the corpus callosum were EGFP-positive.

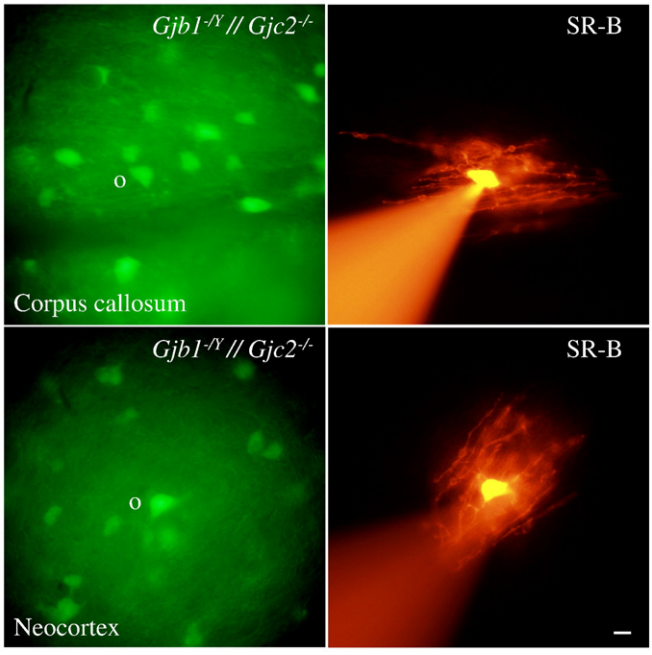

Fig. 6. Absent O:A coupling in the neocortex and corpus callosum of *Gjb1-//Gjc2*-double-null mice. These are images from P24 to P30 of *Gjb1-//Gjc2*-double-null mice (which lack Cx32 and Cx47)—the corpus callosum is shown in the upper panels and the neocortex is shown in the lower panels. An EGFP-positive (FITC filters) oligodendrocyte (o) was patched with an electrode containing SR-B and visualized (TRITC filters) after 20 min. SR-B remains confined to the injected cell, but labels the processes of injected cells. Scale bar: 10μm.

O:A coupling in gray matter

We demonstrated bidirectional O:A coupling in the neocortex for the first time, using three different experimental designs. First, SR-101 labels astrocytes in acute slices, as previously found (Kafitz et al., 2008), but also labels oligodendrocytes. Second, SR-101-positive astrocytes can be labeled by injecting LY into surrounding EGFP-positive oligodendrocytes. Thus, it is likely that at least some of the SR-101-positive "astrocytes" in prior reports likely were, in fact, SR-101-positive oligodendrocytes (Kafitz et al., 2008; Nimmerjahn et al., 2004). Third, when EGFP-positive oligodendrocytes are filled with SR-B, SR-B transfers to surrounding EGFP-negative cells, presumably astrocytes. In all of these experimental designs, Cx47:Cx43 channels likely mediate O:A coupling, as this was not seen in *Gjc2*-null mice (and was seen in *Gjb1*-null mice). We ruled out the possibility that our results were confounded by the impermeability of Cx32:Cx30 channels to SR-101, SR-B, or LY, by labeling EGFP-positive cells with biocytin, which diffused into adjacent cells in $Gjc2^{+/-}$ mice but not in $Gjc2^{-/-}$ mice.

Glial GJ coupling in the CNS

The lack of O:A coupling in double-null $Gjb1^{-/Y}$//$Gjc2^{-/-}$ mice support the model that O:A coupling is solely mediated by two pairs of connexins, Cx47:Cx43 and Cx32:Cx30(Maglione et al., 2010; Orthmann-Murphy et al., 2008; Wallraff et al., 2006) Because the lack of Cx47, but not the lack of Cx43, results in absent O:A coupling (Maglione et al., 2010), it is possible that Cx47 forms a channel with Cx30, as shown *in vitro* (Magnotti et al., 2011), but this remains to be formally demonstrated *in vivo*. Although oligodendrocytes express Cx29 (Altevogt et al., 2002; Altevogt and Paul, 2004b; Sohl et al., 2001), Cx29 does not form functional

channels *in vitro* (Ahn et al., 2008) or *in vivo*, as shown by the complete lack of coupling in double-null $Gjb1^{-/Y}//Gjc2^{-/-}$ mice (Fig. 6; see also (Maglione et al., 2010). Although astrocytes may express Cx26 (Nagy et al., 2003b) but see also (Filippov et al., 2003), and Cx26 can form functional homotypic channels as well as heterotypic channels with Cx30 and Cx32(Oh et al., 1999, Yum et al., 2007) the lack of coupling in mice lacking both Cx30 and Cx43 ((Maglione et al., 2010) indicates that Cx26 does not participate in glial coupling *in vivo*.

The conclusion that "oligodendrocytes shared intercellular gap junctions only with astrocytes, with each oligodendrocyte isolated from other oligodendrocytes except via astrocyte intermediaries" (Rash et al., 2001a,b) was based on freeze-fracture EM, later augmented with immunostaining (Kamasawa et al., 2005; Massa and Mugnaini, 1982; Rash et al., 1997). This conclusion discounted previous reports of GJs between oligodendrocytes (Li et al., 1997; Mugnaini, 1986; Sandri et al., 1982; Sotelo and Angaut, 1973), which we found to be abundant at least in the corpus callosum of mice at the ages we examined. The extent of O:O coupling in other white matter tracts and at older ages remains to be determined.

The role of glial GJ coupling

Two physiological roles of glial GJ coupling have been defined to date: O:A and A:A coupling contribute to the spatial buffering of K^+ released during neural activity (Berger et al., 1991; Chvatal et al., 1999; Frankenhaeuser and Hodgkin, 1956; Kamasawa et al., 2005; Menichella et al., 2006; Orkand et al., 1966; Wallraff et al., 2006), and A:A coupling is essential for metabolic support during neural activity (Rouach et al., 2008). If O:O coupling contributes to these functions, then the CNS manifestations observed in patients with *GJB1* and *GJC2* mutations could result from impaired metabolic support and K^+ buffering (Orthmann-Murphy et al., 2008).

Our results have implications for the pathogenesis of PMLD, which is caused by loss of function mutations of *GJC2* (Orthmann-Murphy et al., 2008). We have previously shown that Cx47 mutants associated with PMLD do not form functional channels with wild type Cx47 or Cx43 (Orthmann-Murphy et al., 2007a), so that these mutants should affect both O:O and O:A coupling. It seems plausible that O:O and O:A coupling are similar in humans, even subserved by the same connexins as in mice, but the relative importance of O:O and O:A coupling in the pathogenesis of PMLD remains to be determined. Given the prominent abnormalities in the white matter of patients with PMLD, one could imagine that O:O coupling in the white matter is more dependent on Cx47 in humans, although we did not find evidence for this in mice. *Gjc2*-null mice, however, may not be an adequate model of PMLD in this regard, as these mice have a mild phenotype; the loss of both Cx32 and Cx47 is needed to produce a severe leukodystrophy in mice (Menichella et al., 2003; Odermatt et al., 2003) equivalent to what is seen in PMLD.

Acknowledgments

This work was supported by the NIH grant NS55284. We thank Dr. Jian Li for help with the electron microscopy, and the Boespflug Foundation for the support.

References

Ahn, M., Lee, J., Gustafsson, A., Enriquez, A., Lancaster, E., Sul, J.Y., Haydon, P.G., Paul, D.L., Huang, Y., Abrams, C.K., Scherer, S.S., 2008. Cx29 and Cx32, two connexins expressed by myelinating glia, do not interact and are functionally distinct. J. Neurosci. Res. 86, 992–1006.

Akimoto, C., Morita, M., Yamamoto, M., Nakano, I., 2010. A novel mutation in X-linked Charcot–Marie–tooth (CMTXI) disease associated with central conduction slowing on brainstem auditory evoked potential (BAEP). Rinsho Shinkeigaku 50, 399–403.

Altevogt, B.M., Paul, D.L., 2004a. Four classes of intercellular channels between glial cells in the CNS. J. Neurosci. 24, 4313–4323.

Altevogt, B.M., Paul, D.L., 2004b. Four classes of intercellular channels between glial cells in the CNS. J. Neurosci. 24, 4313–4323.

Altevogt, B.M., Kleopa, K.A., Postma, F.R., Scherer, S.S., Paul, D.L., 2002. Connexin29 is uniquely distributed within myelinating glial cells of the central and peripheral nervous systems. J. Neurosci. 22, 6458–6470.

Bahr, M., Andres, F., Timmerman, V., Nelis, M.E., Van Broeckhoven, C., Dichgans, J., 1999. Central visual, acoustic, and motor pathway involvement in a Charcot–Marie–Tooth family with an Asn205Ser mutation in the connexin 32 gene. J. Neurol. Neurosurg. Psychiatry 66, 202–206.

Berger, T., Schnitzer, J., Kettenmann, H., 1991. Developmental changes in the membrane current pattern, K+ buffer capacity, and morphology of glial cells in the corpus callosum slice. J. Neurosci. 11, 3008–3024.

Bugiani, M., Al Shahwan, S., Lamantea, E., Bizzi, A., Bakhsh, E., Moroni, I., Balestrini, M.R., Uziel, G., Zeviani, M., 2006. GJA12 mutations in children with recessive hypomyelinating leukoencephalopathy. Neurology 67, 273–279.

Butt, A.M., Ransom, B.R., 1989. Visualization of oligodendrocytes and astrocytes in the intact rat optic nerve by intracellular injection of lucifer yellow and horseradish peroxidase. Glia 2, 470–475.

Chvatal, A., Anderova, M., Ziak, D., Sykova, E., 1999. Glial depolarization evokes a larger potassium accumulation around oligodendrocytes than around astrocytes in gray matter of rat spinal cord slices. J. Neurosci. Res. 56, 493–505.

Emsley, J.G., Macklis, J.D., 2006. Astroglial heterogeneity closely reflects the neuronal-defined anatomy of the adult murine CNS. Neuron Glia Biol. 2, 175–186.

Filippov, M.A., Hormuzdi, S.G., Fuchs, E.C., Monyer, H., 2003. A reporter allele for investigating connexin 26 gene expression in the mouse brain. Eur. J. Neurosci. 18, 3183–3192.

Frankenhaeuser, B., Hodgkin, A.L., 1956. The after-effects of impulses in the giant nerve fibres of Loligo. J. Physiol. 131, 341–376.

Haas, B., Schipke, C.G., Peters, O., Sohl, G., Willecke, K., Kettenmann, H., 2006. Activity-dependent ATP-waves in the mouse neocortex are independent from astrocytic calcium waves. Cereb. Cortex 16, 237–246.

Houades, V., Rouach, N., Ezan, P., Kirchhoff, F., Koulakoff, A., Giaume, C., 2006. Shapes of astrocyte networks in the juvenile brain. Neuron Glia Biol. 2, 3–14.

Houades, V., Koulakoff, A., Ezan, P., Seif, I., Giaume, C., 2008. Gap junction-mediated astrocytic networks in the mouse barrel cortex. J. Neurosci. 28, 5207–5217.

Imamoto, K., Paterson, J.A., Leblond, C.P., 1978. Radioautographic investigation of gliogenesis in the corpus callosum of young rats. I. Sequential changes in oligodendrocytes. J. Comp. Neurol. 180 (115–28), 132–137.

Kafitz, K.W., Meier, S.D., Stephan, J., Rose, C.R., 2008. Developmental profile and properties of sulforhodamine 101—labeled glial cells in acute brain slices of rat hippocampus. J. Neurosci. Methods 169, 84–92.

Kamasawa, N., Sik, A., Morita, M., Yasumura, T., Davidson, K.G., Nagy, J.I., Rash, J.E., 2005. Connexin-47 and connexin-32 in gap junctions of oligodendrocyte somata, myelin sheaths, paranodal loops and Schmidt–Lanterman incisures: implications for ionic homeostasis and potassium siphoning. Neuroscience 136, 65–86.

Kleopa, K.A., Scherer, S.S., 2006. Molecular genetics of X-linked Charcot–Marie–Tooth disease. Neuromolecular Med. 8, 107–122.

Kleopa, K.A., Yum, S.W., Scherer, S.S., 2002. Cellular mechanisms of connexin32 mutations associated with CNS manifestations. J. Neurosci. Res. 68, 522–534.

Kleopa, K.A., Orthmann, J.L., Enriquez, A., Paul, D.L., Scherer, S.S., 2004. Unique distributions of the gap junction proteins connexin29, connexin32, and connexin47 in oligodendrocytes. Glia 47, 346–357.

Kleopa, K.A., Zamba-Papanicolaou, E., Alevra, X., Nicolaou, P., Georgiou, D.M., Hadjisavvas, A., Kyriakides, T., Christodoulou, K., 2006. Phenotypic and cellular expression of two novel connexin32 mutations causing CMT1X. Neurology 66, 396–402.

Kumar, N.M., Gilula, N.B., 1996. The gap junction communication channel. Cell 84, 381–388.

Li, J., Hertzberg, E.L., Nagy, J.I., 1997. Connexin32 in oligodendrocytes and association with myelinated fibers in mouse and rat brain. J. Comp. Neurol. 379, 571–591.

Li, X., Ionescu, A.V., Lynn, B.D., Lu, S., Kamasawa, N., Morita, M., Davidson, K.G., Yasumura, T., Rash, J.E., Nagy, J.I., 2004. Connexin47, connexin29 and connexin32 co-expression in oligodendrocytes and Cx47 association with zonula occludens-1 (ZO-1) in mouse brain. Neuroscience 126, 611–630.

Li, X., Penes, M., Odermatt, B., Willecke, K., Nagy, J.I., 2008. Ablation of Cx47 in transgenic mice leads to the loss of MUPP1, ZONAB and multiple connexins at oligodendrocyte–astrocyte gap junctions. Eur. J. Neurosci. 28, 1503–1517.

Maglione, M., Tress, O., Haas, B., Karram, K., Trotter, J., Willecke, K., Kettenmann, H., 2010. Oligodendrocytes in mouse corpus callosum are coupled via gap junction channels formed by connexin47 and connexin32. Glia 58, 1104–1117.

Magnotti, L.M., Goodenough, D.A., Paul, D.L., 2011. Functional heterotypic interactions between astrocyte and oligodendrocyte connexins. Glia 59, 26–34.

Massa, P.T., Mugnaini, E., 1982. Cell junctions and intramembrane particles of astrocytes and oligodendrocytes: a freeze-fracture study. Neuroscience 7, 523–538.

Matyash, V., Kettenmann, H., 2010. Heterogeneity in astrocyte morphology and physiology. Brain Res. Rev. 63, 2–10.

Menichella, D.M., Goodenough, D.A., Sirkowski, E., Scherer, S.S., Paul, D.L., 2003. Connexins are critical for normal myelination in the CNS. J. Neurosci. 23, 5963–5973.

Menichella, D.M., Majdan, M., Awatramani, R., Goodenough, D.A., Sirkowski, E., Scherer, S.S., Paul, D.L., 2006. Genetic and physiological evidence that oligodendrocyte gap junctions contribute to spatial buffering of potassium released during neuronal activity. J. Neurosci. 26, 10984–10991.

Mugnaini, E., 1986. In: Fedoroff, S., Vernadakis, A. (Eds.), Astrocytes. Academic Press, Orlanodo Florida, pp. 329–371.

Nagy, J.I., Rash, J.E., 2003. Astrocyte and oligodendrocyte connexins of the glial syncytium in relation to astrocyte anatomical domains and spatial buffering. Cell Commun. Adhes. 10, 401–406.

Nagy, J.I., Ionescu, A.V., Lynn, B.D., Rash, J.E., 2003a. Coupling of astrocyte connexins Cx26, Cx30, Cx43 to oligodendrocyte Cx29, Cx32, Cx47: implications from normal and connexin32 knockout mice. Glia 44, 205–218.

Nagy, J.I., Ionescu, A.V., Lynn, B.D., Rash, J.E., 2003b. Coupling of astrocyte connexins Cx26, Cx30, Cx43 to oligodendrocyte Cx29, Cx32, Cx47: implications from normal and connexin32 knockout mice. Glia 44, 205–218.

Nelles, E., Butzler, C., Jung, D., Temme, A., Gabriel, H.D., Dahl, U., Traub, O., Stumpel, F., Jungermann, K., Zielasek, J., Toyka, K.V., Dermietzel, R., Willecke, K., 1996. Defective propagation of signals generated by sympathetic nerve stimulation in the liver of connexin32-deficient mice. Proc. Natl. Acad. Sci. USA 93, 9565–9570.

Nicholson, G., Corbett, A., 1996. Slowing of central conduction in X-linked Charcot–Marie–Tooth neuropathy shown by brain stem auditory evoked responses. J. Neurol. Neurosurg. Psychiatry 61, 43–46.

Nicholson, G.A., Yeung, L., Corbett, A., 1998. Efficient neurophysiologic selection of X-linked Charcot–Marie–Tooth families: ten novel mutations. Neurology 51, 1412–1416.

Nimmerjahn, A., Kirchhoff, F., Kerr, J.N., Helmchen, F., 2004. Sulforhodamine 101 as a specific marker of astroglia in the neocortex in vivo. Nat. Methods 1, 31–37.

Odermatt, B., Wellershaus, K., Wallraff, A., Seifert, G., Degen, J., Euwens, C., Fuss, B., Bussow, H., Schilling, K., Steinhauser, C., Willecke, K., 2003. Connexin 47 (Cx47)-deficient mice with enhanced green fluorescent protein reporter gene reveal predominant oligodendrocytic expression of Cx47 and display vacuolized myelin in the CNS. J. Neurosci. 23, 4549–4559.

Oh, S., Rubin, J.B., Bennett, M.V., Verselis, V.K., Bargiello, T.A., 1999. Molecular determinants of electrical rectification of single channel conductance in gap junctions formed by connexins 26 and 32. J. Gen. Physiol. 114, 339–364.

Orkand, R.K., Nicholls, J.G., Kuffler, S.W., 1966. Effect of nerve impulses on the membrane potential of glial cells in the central nervous system of amphibia. J. Neurophysiol. 29, 788–806.

Orthmann-Murphy, J.L., Enriquez, A.D., Abrams, C.K., Scherer, S.S., 2007a. Loss-of-function GJA12/Connexin47 mutations cause Pelizaeus–Merzbacher-like disease. Mol. Cell. Neurosci. 34, 629–641.

Orthmann-Murphy, J.L., Freidin, M., Fischer, E., Scherer, S.S., Abrams, C.K., 2007b. Two distinct heterotypic channels mediate gap junction coupling between astrocyte and oligodendrocyte connexins. J. Neurosci. 27, 13949–13957.

Orthmann-Murphy, J.L., Abrams, C.K., Scherer, S.S., 2008. Gap junctions couple astrocytes and oligodendrocytes. J. Mol. Neurosci. 35, 101–116.

Panas, M., Kalfakis, N., Karadimas, C., Vassilopoulos, D., 2001. Episodes of generalized weakness in two sibs with the C164T mutation of the connexin 32 gene. Neurology 57, 1906–1908.

Pastor, A., Kremer, M., Moller, T., Kettenmann, H., Dermietzel, R., 1998. Dye coupling between spinal cord oligodendrocytes: differences in coupling efficiency between gray and white matter. Glia 24, 108–120.

Paulson, H.L., Garbern, J.Y., Hoban, T.F., Krajewski, K.M., Lewis, R.A., Fischbeck, K.H., Grossman, R.I., Lenkinski, R., Kamholz, J.A., Shy, M.E., 2002. Transient central nervous system white matter abnormality in X-linked Charcot–Marie–Tooth disease. Ann. Neurol. 52, 429–434.

Peters, A., Palay, S., Webster, H., 1991. Fine Structure of the Nervous System: Neurons and Their Supporting Cells. Oxford University Press, NewYork, NY.

Ransom, B.R., Kettenmann, H., 1990. Electrical coupling, without dye coupling, between mammalian astrocytes and oligodendrocytes in cell culture. Glia 3, 258–266.

Rash, J.E., Duffy, H.S., Dudek, F.E., Bilhartz, B.L., Whalen, L.R., Yasumura, T., 1997. Grid-mapped freeze-fracture analysis of gap junctions in gray and white matter of adult rat central nervous system, with evidence for a "panglial syncytium" that is not coupled to neurons. J. Comp. Neurol. 388, 265–292.

Rash, J.E., Yasumura, T., Davidson, K.G., Furman, C.S., Dudek, F.E., Nagy, J.I., 2001a. Identification of cells expressing Cx43, Cx30, Cx26, Cx32 and Cx36 in gap junctions of rat brain and spinal cord. Cell Commun. Adhes. 8, 315–320.

Rash, J.E., Yasumura, T., Dudek, F.E., Nagy, J.I., 2001b. Cell-specific expression of connexins and evidence of restricted gap junctional coupling between glial cells and between neurons. J. Neurosci. 21, 1983–2000.

Rouach, N., Koulakoff, A., Abudara, V., Willecke, K., Giaume, C., 2008. Astroglial metabolic networks sustain hippocampal synaptic transmission. Science 322, 1551–1555.

Sandri, C., Van Buren, J.M., Akert, K., 1982. Membrane morphology of the vertebrate nervous system. Prog. Brain Res. 46, 201–265.

Siskind, C., Feely, S.M., Bernes, S., Shy, M.E., Garbern, J.Y., 2009. Persistent CNS dysfunction in a boy with CMT1X. J. Neurol. Sci. 279, 109–113.

Sohl, G., Willecke, K., 2004. Gap junctions and the connexin protein family. Cardiovasc. Res. 62, 228–232.

Sohl, G., Eiberger, J., Jung, Y.T., Kozak, C.A., Willecke, K., 2001. The mouse gap junction gene connexin29 is highly expressed in sciatic nerve and regulated during brain development. Biol. Chem. 382, 973–978.

Sotelo, C., Angaut, P., 1973. The fine structure of the cerebellar central nuclei in the cat. I. Neurons and neuroglial cells. Exp. Brain Res. 16, 410–430.

Takashima, H., Nakagawa, M., Umehara, F., Hirata, K., Suehara, M., Mayumi, H., Yoshishige, K., Matsuyama, W., Saito, M., Jonosono, M., Arimura, K., Osame, M., 2003. Gap junction protein beta 1 (GJB1) mutations and central nervous system symptoms in X-linked Charcot–Marie–Tooth disease. Acta Neurol. Scand. 107, 31–37.

Taylor, R.A., Simon, E.M., Marks, H.G., Scherer, S.S., 2003. The CNS phenotype of X-linked Charcot–Marie–Tooth disease: more than a peripheral problem. Neurology 61, 1475–1478.

Uhlenberg, B., Schuelke, M., Ruschendorf, F., Ruf, N., Kaindl, A.M., Henneke, M., Thiele, H., Stoltenburg-Didinger, G., Aksu, F., Topaloglu, H., Nurnberg, P., Hubner, C., Weschke, B., Gartner, J., 2004. Mutations in the gene encoding gap junction protein alpha 12 (connexin 46.6) cause Pelizaeus–Merzbacher-like disease. Am. J. Hum. Genet. 75, 251–260.

Wallraff, A., Kohling, R., Heinemann, U., Theis, M., Willecke, K., Steinhauser, C., 2006. The impact of astrocytic gap junctional coupling on potassium buffering in the hippocampus. J. Neurosci. 26, 5438–5447.

Yum, S.W., Zhang, J., Valiunas, V., Kanaporis, G., Brink, P.R., White, T.W., Scherer, S.S., 2007. Human connexin26 and connexin30 form functional heteromeric and heterotypic channels. Am. J. Physiol. Cell Physiol. 293, C1032–C1048.

Zambelis, T., Panas, M., Kokotis, P., Karadima, G., Kararizou, E., Karandreas, N., 2008. Central motor and sensory pathway involvement in an X-linked Charcot–Marie–Tooth family. Acta Neurol. Belg. 108, 44–47.